CHEMICAL ENGINEERING TRANSACTIONS
VOL. 99, 2023

A publication of AIDIC
The Italian Association of Chemical Engineering
Online at www.cetjournal.it

Guest Editors: Sauro Pierucci, Flavio Manenti

ISBN 978-88-95608-98-3; **ISSN** 2283-9216

DOI: 10.3303/CET2399025

Hydrodynamic Cavitation for Pollutant Treatment in the New Horizon of Green Chemistry

Anna Stoppato[a], Alberto Benato[a], Francesco De Vanna[a*], Graziano Tassinato[b], Francesco Nisato[b]

[a]Department of Industrial Engineering, University of Padova, Via Venezia, 1, 35121, Italy
[b]Green Propulsion Laboratory – Gruppo Veritas SpA, Venezia, Italy
francesco.devanna@unipd.it

The study describes a systematic numerical optimization of a Venturi tube for wastewater treatment under cavitation conditions. The numerical approach employs computational fluid dynamics methodologies in a Reynolds-Averaged Navier-Stokes framework combined with an optimization algorithm to enhance a baseline Venturi geometry. A robust meshing technique is provided in order to define the numerical model associated with the baseline solution. The process compares alternative mesh sizes and turbulence closure to discover the optimal accuracy and processing time balance. Then the model is used as a starting point for the optimization. An optimal configuration is found to be able to improve the tube mean vapor quality by around 130% compared to the starting geometry.

1. Introduction

Hydrodynamic cavitation is a well-known phenomenon that is gaining prominence owing to its use in various technical and chemical processes, such as emulsification, oxidation, nanomaterial production, and wastewater treatment. Hydrodynamic cavitation aims to induce cavitating microbubbles, and the Venturi tube is a commonly used device for this purpose. A Venturi tube is a basic and widely used fluid device that consists of a converging section where the flow is accelerated, a throat zone where the pressure reaches its lowest value, and a diverging segment where the tube recovers the cross-section of the pipe in which it is placed. If the ratio between the throat diameter of the Venturi and the diameter of the external pipe is low enough, the velocity increment induced by the section reduction can lead to cavitating conditions in the throat flow. When the static pressure falls below the vapor pressure, cavitation is defined as the development, growth, and collapse of microbubbles or vapor cavities in a liquid. Due to the adiabatic compression of the cavities, the collapse happens at various points. Consequently, a substantial amount of energy is quickly released, resulting in the production of a super-critical state with high temperature and pressure (5000 K and 500 bar) similar to those on the solar surface. These conditions accelerate chemical and physical transformations, which can be utilized for a variety of practical applications, including the destruction of chemical contaminants in wastewater treatment (Gogate et al. 2009, Dular et al. 2012, Šarc et al. 2018).
Carpenter et al. 2017 summed up the theory about cavitation; in particular, the hotspots of collapsing cavities, and discussed the many approaches to generate the multi-phase phenomena and the corresponding uses of the technology in different contexts. The research emphasized the significance of specific geometric characteristics of the Venturi tube. Using Computational Fluid Dynamics (CFD) techniques, Dastane et al. 2019 numerically analysed cavitating flow in a Venturi tube, comparing various mesh sizes and performing single- and multi-phase simulations. They observed that the single-phase method underestimates the value of the input pressure. Bashir et al. 2011 offer a CFD-based optimization technique for cavitating Venturi tubes' most crucial geometrical parameters. Using tests and simulations, Li et al. 2019 explore the impact of Venturi geometries on cavitation. However, the prediction of cavitating flows using computational methods is still a critical issue, and only few results are available in the literature.

Paper Received: 30 November 2022; Revised: 20 March 2023; Accepted: 29 April 2023
Please cite this article as: Stoppato A., Benato A., De Vanna F., Tassinato G., Nisato F., 2023, Hydrodynamic Cavitation for Pollutant Treatment in the New Horizon of Green Chemistry, Chemical Engineering Transactions, 99, 145-150 DOI:10.3303/CET2399025

In particular, the most advanced CFD strategies, such as Large-Eddy Simulations (LES) and Direct Numerical Simulations (DNS), can hardly be adopted in multi-phase and complex flow conditions, such as those about a deep cavitating wall-bounded flow. Therefore, digital prototyping of such devices is still demanded by Reynolds-Averaged Navier-Stokes (RANS) based models, albeit with all the limitations that such strategy embeds.
The present work aims to determine the most critical parameters influencing RANS CFD modelling results for flow cavitation inside Venturi tubes and to provide optimization suggestions for enhancing a baseline Venturi design. A RANS model has been built and used to predict the two-phase flow, and to make a comparison between various model resolutions in terms of grid discretization level. The results indicate that high grid resolutions are required for numerically insensitive outcomes. Finally, the baseline model is used as a starting point for an optimization procedure devoted to find a novel design of the tube capable of improving the steam generation.
The paper is organized as follows: Section 2 presents the numerical model and provides a description of the numerical settings. Section 3 summarizes and discusses the mesh sensitivity analysis with the aim of looking to the optimal mesh size. Section 4 provides hints concerning the Latin Hypercube Sampling (LHS) method and gives quantitative information concerning optimal geometry configurations of the tube. Finally, in Section 5 concluding remarks are given.

2. Computational setup

Figure 1 shows the scheme of the analysed geometry together with geometrical dimensions.
The Venturi tube has a throat diameter (d) of 3.18 mm, while the pipe diameter (D) is equal to 12.7 mm. The converging angle slopes is of 19° and the diverging angle is equal to 5°. The CFD model is extended by 30 mm and 80 mm before and after the L_1 and L_5 segments to achieve a fully developed turbulent flow and prevent unphysical recirculations. The axial symmetry of the tube limited the task to a 2D domain. The model reproduces the experimental setup presented by Shi et al. 2019. Ansys-Workbench 2020 R1 is used to build up the geometry and the grids, while Ansys-Fluent is employed to solve the flow field.

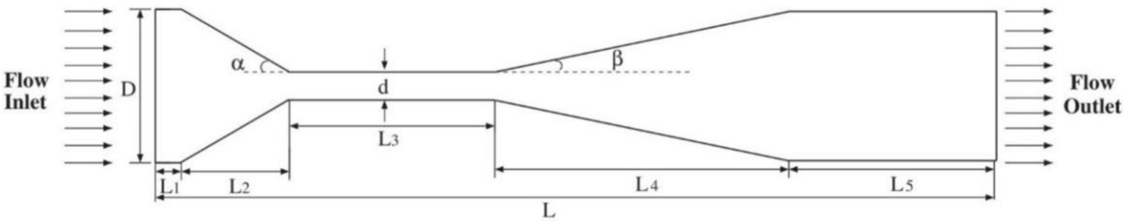

Figure 1: Schematic view of the Venturi tube geometry. Geometrical dimensions are listed in Table 1.

Table 1: Geometry specifications of the Venturi cavitating tube

D (mm)	d (mm)	L_2 (mm)	L_3 (mm)	L_4 (mm)	L_5 (mm)	alpha	beta
12.7	3.18	6.0	14.0	54.0	6.0	19.0	5.0

Three structured meshes of 100’000 (100k), 200’000 (200k) and 300’000 (300k) elements have been built and tested. Adopting the internal software suites, each computational grid is quality validated to ensure a maximum skewness value below 0.22, an inflation growth rate between 1.05 and 1.20, and an orthogonality quality value above 0.99. The inflation is placed close to the walls to improve resolution in the boundary layer and ensure that the wall Y plus (y+) values are accurate. Specifically, the aim is to address a y+ value lower than 1. Table 2 gives more information on the mesh properties, while Figure 2 shows a zoom of the extra-fine mesh in the area around the Venturi inflowing corner.

Table 2: Grid quality parameters

MESH	Mean Aspect Ratio	Mean Skewness	Mean Orthogonal Quality
100k	4.194	2.80×10^{-2}	0.996
200k	4.508	2.73×10^{-2}	0.996
300k	6.091	2.21×10^{-2}	0.997

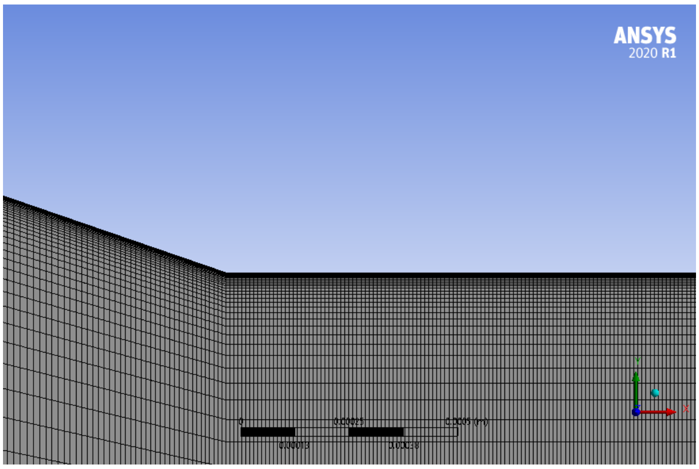

Figure 2: Detailed view of the 200k mesh in the inflowing Venturi corner.

The system's dynamics is simulated by finding solutions to an incompressible RANS system of equations in a steady-state framework. The flow field dynamics is solved accordingly with four turbulence models. The model complexity rises progressively from the first to the last and all of them are compared during the analysis to find the best compromise between accuracy and calculation time. To be more specific, the following models have been selected and utilizes: the one equation Spalart-Allmaras (SA) model, the two equations k-epsilon realizable model, the two equations k-omega Shear Stress Transport (SST) model, and the four equations Transition SST (TSST) model. To solve the mass and momentum conservation equations related to the behaviour of the cavitating flow in the mixture model, the pressure-velocity coupled method is used. Thus, to satisfy the requirements of the coupling algorithms, the equations include implicit discretization of the pressure gradient terms and the mass flow. To discretize the convective components in the transport equations for the vapor volume fraction, the Quadratic Upwind Interpolation for Convection Kinematics (QUICK) technique is used. The PREssure STaggering Option (PRESTO) method is adopted in the computation of the pressure. To discretize the convection terms that are included in the momentum equations, the second-order upwind technique is selected. Finally, to mimic cavitating two-phase flows for the multiphase flow solutions, the mixture model is used (water-vapor). The phase transition is computed according to the Schnerr-Sauer cavitation model. As boundary conditions, "pressure inlet" and "pressure outlet" conditions are enforced at the inflowing and outflowing edges, respectively; this means setting the total and the static pressure. Additionally, "adiabatic no-slip wall" conditions are enforced at the Venturi internal surfaces. At nameplate point, a condition that embeds cavitating events in the throat of the tube is set. This means total pressure of 180'000 Pa at the inflow and a static pressure of 101'325 Pa at the outflow, respectively.

3. Model validation

First, a mesh sensitivity analysis has been conducted with the total intake pressure set to its design value of 180 kPa. This setting ensures proper operation under cavitating conditions. Global parameters are compared to fine-tune the grid and assess how the numerical discretization level influences the findings. Figure 3 depicts the non-dimensional Venturi pressure drop and coarse-scaled drag force as a function of the grid resolution. The 100k element mesh somewhat underestimates the drop in pressure, but the model saturates the value after 200k grid refinements. Instead, the drag coefficient data are exactly matched as the grid size changes. This implies that an excessive number of mesh elements would be unreasonable, which would only result in stressing computer resources.. Based on the evaluation of the global parameters, the 200k configuration seems to be the ideal trade-off between numerical accuracy and computing load. Thus, the 200k mesh arrangement, combined with the k-omega SST, is selected and used for the upcoming analyses.

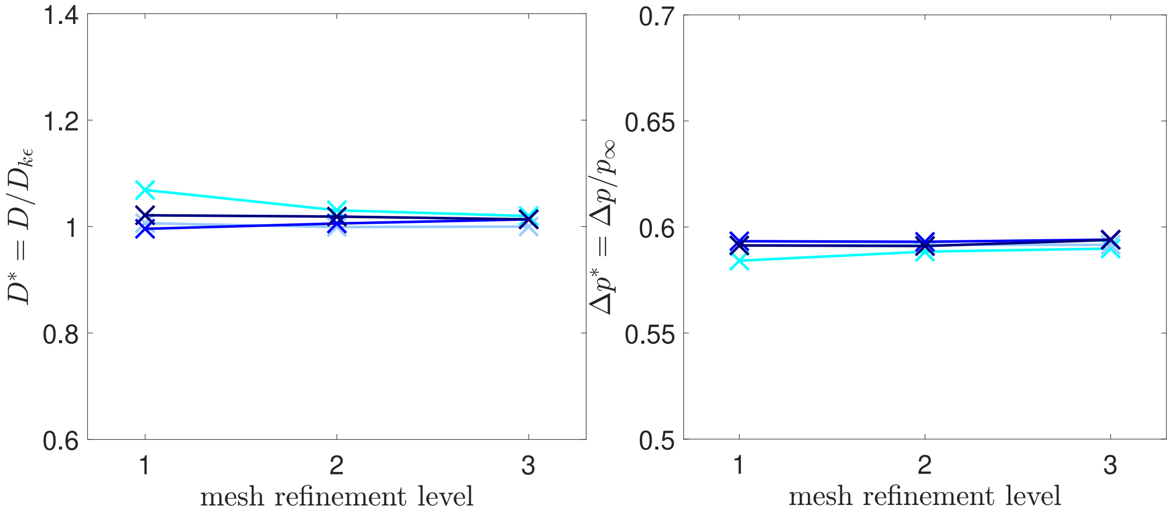

Figure 3: Model validation as a function of the grid refinement and turbulence model. From lighter to darker tones colours refer to gradually more complex turbulence models, i.e, SA, k-epsilon realizable, k-omega SST and TSST, respectively. Refinement level refers to the 100k, 200k, and 300k mesh, respectively.

4. Latin Hypercube Sampling and optimization results

In this work, the LHS technique is employed to design improved Venturi geometries concerning a priori specified goals. The LHS technique has been proposed by McKay et al. 2000 as a sampling mechanism for filling a design variable space. The importance of sampling derives from the need to correctly choose the input variables of a mathematical model describing real occurrences, thereby gathering the necessary information about the probability distribution of the output with the fewest number of inputs. Swiler et al. (2004) define Latin hypercube sampling as a technique for examining the probability distribution of a multivariate function with *k* variables by selecting *n* different values for each variable. Using equal probability reasoning, the values are selected by dividing each variable into *n* different pieces. As a result, after randomly picking one value from each layer, the values collected for each variable are randomly paired, producing *n* evaluations of the input variables. Loh (1996) provides a more detailed examination of the theoretical background of the LHS approach, as well as the method's fundamental mathematical formulation. As reported by Helton et al. (2003), this technique has been widely used in complex system analyses, with its main characteristics highlighted, such as its simplicity and ability to result in more uniform stratification than other random sampling strategies, revealing to be a suitable method for selecting input variables or having a rough estimation of the optimal locations. The Latin Hypercube Sampling technique is employed in this study by using the Matlab "lhsdesign" function, which generates a Latin Hypercube Sample matrix of size *k x n*, where *k* and *n* have the previously mentioned meanings. In particular, each configuration produced by the LHS method consists of a variation of the baseline solution reconstructed through Beziér splines. The approach allows obtaining different Venturi tube geometries in terms of shape angles, inlet, throat, and discharge lengths, as well as it ensures a smooth profile of the tube.
To assess the performance of the Venturi pipe geometric configurations in terms of their capability of generating cavitation events, to each configuration has been assigned a performance parameter relating to the generation of steam in the pipe's discharge portion. Five stations (named as stat1, stat2, stat3, stat4, stat5) are placed beside the tube discharging section to sample the radial distribution of the vapor quality. The average integral value of the steam quality, X_v, is derived for each distribution. As a result, this value indicates how much steam is linked with each station. Finally, the five measurements associated with each station are averaged to provide a single performance parameter for each geometric arrangement. When applied to the baseline setup, this method produces a performance metric of $X_v = 0.1421$. Instead, the LHS optimization process yields a set of 12 configurations capable of greatly enhancing the performance inherent in steam generation compared to the baseline, as listed in Table 3.
Even though all the factors considered result in a significant boost in steam production performance, individual 6 is unquestionably the best. In fact, it is observed a 133% increase in the steam generation on average when compared to the baseline solution. Figure 4 compares the steam quality trend at the 5 stations for configuration 6 to the same data acquired in the baseline situation. The solid curves represent the optimal case, while the dash-dotted curves report the baseline solution. In Figure 4, *r* and *R* denote the radial coordinate and the maximum radius associated to each station, respectively.

It is also observed that the baseline configuration tends to cluster the vapor production in the early stations, with the first station having a clear advantage. Furthermore, the baseline solution's stations 1 and 2 (in Figure 4 named as stat1 and stat2) concentrate vapor quality along the pipe wall. Instead, the optimal solution not only improves steam distribution in stations 1 and 2, but also generates a significant amount of steam in stations 3 and 4 (in Figure 4 named as stat3 and stat4), whereas the baseline does not. For the sake of completeness, it is feasible to claim that stations with vapor quality less than 10^{-2} are not meaningful and, so, they are not reported.

Table 3: Resume of the optimization analysis

Configuration	Vapour performance index	Improvement [%]
baseline	0.1421	-
1	0.2688	89.11
2	0.2382	67.59
3	0.2825	98.75
4	0.1734	22.01
5	0.1933	36.02
6	0.3321	133.7
7	0.2138	50.40
8	0.1627	14.48
9	0.1455	2.38
10	0.2275	60.05
11	0.1931	35.88
12	0.1451	2.10

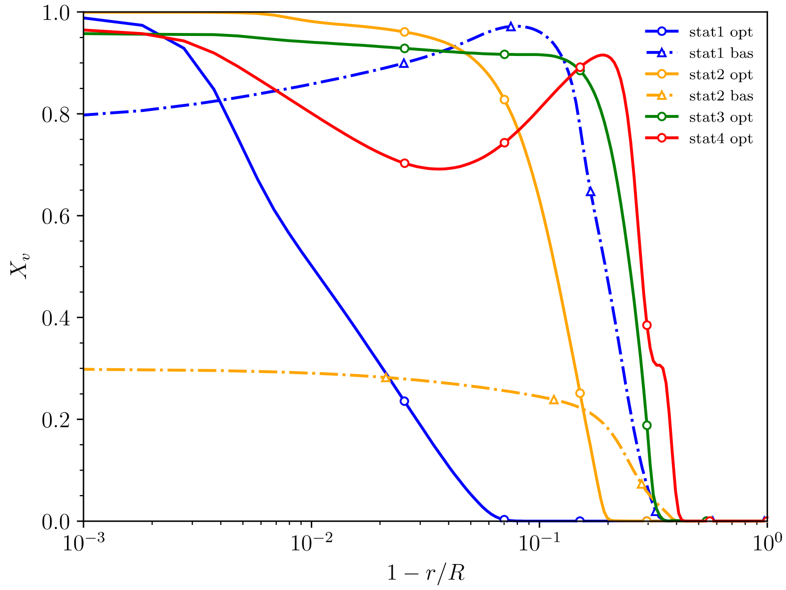

Figure 4: Baseline and optimal solutions comparison in terms of steam production distribution in the Venturi discharging sections.

5. Conclusions

The present work investigates a baseline and an improved Venturi tube layout for hydrodynamic cavitation applications. Firstly, a numerical model is adjusted as a function of grid resolution and turbulence model, with an emphasis on the findings' independence from mesh refinement.

The baseline model is then employed as a leading configuration in an automated optimization technique based on the LHS method. Compared to the baseline Venturi layout, the procedure can boost the tube's steam output by more than 130%. Furthermore, the enhanced design focuses steam production around the channel axis, while the baseline generates steam production towards the wall. This research demonstrates that optimizing the Venturi tube design can increase the performance of the hydrodynamic system. The optimized device can be used profitably for the purification and disposal of pollutants in water systems without the aid of chemical components, solvents and/or other artificial additives. In future work, experimental campaigns on both baseline and optimize configurations will be conducted with the aim of validating the numerical results and/or develop new and more efficient configurations of the Venturi tube. Optimizations and numerical simulations will be also used to exploit alternative layouts involving multiple venturi tubes or non-symmetrical nozzles.

References

Bashir, T. A., Soni, A. G., Mahulkar, A. V., Pandit, A. B., 2011. The CFD driven optimisation of a modified venturi for cavitational activity. The Canadian Journal of Chemical Engineering, 89(6), 1366-1375.

Carpenter, J., Badve, M., Rajoriya, S., George, S., Saharan, V. K., Pandit, A. B., 2017. Hydrodynamic cavitation: an emerging technology for the intensification of various chemical and physical processes in a chemical process industry. Reviews in Chemical Engineering, 33(5), 433-468.

Dastane, G. G., Thakkar, H., Shah, R., Perala, S., Raut, J., Pandit, A. B., 2019. Single and multiphase CFD simulations for designing cavitating venturi. Chemical Engineering Research and Design, 149, 1-12.

Dular, M., Khlifa, I., Fuzier, S., Adama Maiga, M., Coutier-Delgosha, O., 2012. Scale effect on unsteady cloud cavitation. Experiments in fluids, 53, 1233-1250.

Gogate, P. R., Kabadi, A. M., 2009. A review of applications of cavitation in biochemical engineering/biotechnology. Biochemical Engineering Journal, 44(1), 60-72.

Helton, J. C., Davis, F. J., 2003. Latin hypercube sampling and the propagation of uncertainty in analyses of complex systems. Reliability Engineering & System Safety, 81(1), 23-69.

Li, M., Bussonnière, A., Bronson, M., Xu, Z., Liu, Q., 2019. Study of Venturi tube geometry on the hydrodynamic cavitation for the generation of microbubbles. Minerals Engineering, 132, 268-274.

Loh, W. L., 1996. On Latin hypercube sampling. The annals of statistics, 24(5), 2058-2080.

McKay, M. D., Beckman, R. J., Conover, W. J., 2000. A comparison of three methods for selecting values of input variables in the analysis of output from a computer code. Technometrics, 42(1), 55-61.

Šarc, A., Kosel, J., Stopar, D., Oder, M., Dular, M., 2018. Removal of bacteria Legionella pneumophila, Escherichia coli, and Bacillus subtilis by (super) cavitation. Ultrasonics sonochemistry, 42, 228-236.

Shi, H., Li, M., Nikrityuk, P., Liu, Q., 2019. Experimental and numerical study of cavitation flows in venturi tubes: From CFD to an empirical model. Chemical Engineering Science, 207, 672-687.

Swiler, L. P., Wyss, G. D., 2004. A user's guide to Sandia's latin hypercube sampling software: LHS UNIX library/standalone version (No. SAND2004-2439). Sandia National Laboratories (SNL), Albuquerque, NM, and Livermore, CA (United States).